COMMUNICATION

The effect of the size of surface Pd island ensembles on electron transfer of adsorbed perchlorate ions on Au(111)†

Chen Wu,‡[a] Feng Xu,‡[b] Martin R. Castell[a] and S. C. Edman Tsang*[b]

A progressive increase in the size of Pd ensembles on a mica-supported Au(111) single crystal surface can facilitate electron transfer of perchlorate ions at lower anodic potential in CV curves than pure Au(111) due to a strong ligand effect and Pd–Au neighbouring pairs at edge sites render a higher degree of electron transfer.

Bimetallic nanoparticles can show a more superior activity, selectivity and stability compared to monometallic nanoparticles in various catalytic, electro-catalytic and sensing reactions due to the beneficial synergistic effects of two metal species.[1,2] In particular, Pd–Au bimetallic systems have recently received much attention because of their fascinating catalytic properties in a number of important reactions such as alcohol oxidation, H_2O_2 synthesis, toluene oxidation, vinyl acetate manufacture and electrochemical oxidation in fuel cells.[3–8] Geometric (ensemble), electronic and bifunctional effects have been proposed to explain the improvement in catalyst performance.[7–9] However the influences of bimetallic structure and the synergistic surface combination in catalysis are still under debate. This could be partly due to the fact that the chemical composition, morphology, and electronic structure of bimetallic nanoparticles are markedly affected by preparation methods and experimental conditions. A variety of preparation techniques such as impregnation, co-precipitation and electro-deposition as well as a wide range of testing conditions have been used and compared.[3–9] In addition, the lack of tailoring of the local atomic arrangement at the surface, both for real catalysts and for model systems, has lead to ambiguous conclusions. As a result, Goodman *et al.* performed a carefully controlled deposition of Pd on single crystals of Au(100) and Au(111) and concluded that isolated Pd atoms on the PdAu surface can facilitate coupling between ethylene species and acetate in vinyl acetate synthesis.[7] Similarly, by controlling electro-deposition of Pd onto Au(111) electrodes Maroun *et al.* found the small Pd ensembles

to be more active than the monolayer (ML) Pd films in electro-oxidation of CO.[8] It is noted that a majority of the previous research was on the investigation of the activity of surface Pd atoms modified by Au since Pd atoms are more active than Au in those selected reactions.

Here, we have adopted vapour deposition of Pd on mica-supported Au(111) single crystal surfaces monitored by scanning tunnelling microscopy (STM). We undertook a controlled preparation of bimetallic structures with well-defined surface composition and flat topography. This allowed us to accurately determine the sizes of surface Pd island ensembles on Au(111). Cyclic voltammetry (CV) was also employed to monitor the electronic properties of the surface atoms at room temperature, which in recent years has provided remarkable sensitivity for characterization and resolution of sub-monolayer chemical processes at electrodes. We have chosen to monitor the electron transfer process of perchlorate ions by CV measurements, which takes place only on Au atoms on the anode surface within the scan range, but this time, the Au atoms are modified by controlled surface Pd islands of different sizes.

The details of controlled Pd deposition, STM characterization of mica-supported Au(111) single crystals and the significance of this metal deposition can be found in the ESI.† A clean $(22 \times \sqrt{3})$ Au(111) surface was confirmed by STM prior to Pd deposition. Experiments[8] and calculations[10,11] show that surface segregation can create Au rich surface atoms on Pd deposited Au(111) and Au(001) after heat treatment. Thus, Pd was vapour deposited at room temperature on the gold substrates in a UHV from an electron beam evaporator with no post-annealing so as to reduce gold atom migration. Fig. 1 shows STM images that reveal the evolution of Pd atoms on Au(111) with increasing Pd coverage. The surface area shown is $50 \times 50 \text{ nm}^2$ (for comparison $100 \times 100 \text{ nm}^2$ images are shown in the ESI†). It is known that unreconstructed Au(111) planes consist of hexagonal lattices as Au is an fcc (face centred cubic) crystal. The typical clean Au(111) crystals in UHV should exhibit surface reconstruction, where the atoms in the Au surface layer are contracted uniaxially by $\sim 4\%$ along the $\langle 1\bar{1}0 \rangle$ direction, giving rise to a complex structure of the topmost layer, the so-called herringbone reconstruction with $(22 \times \sqrt{3})$ unit cells. The background herringbone pattern of all our STM

[a] *Department of Materials, University of Oxford, Oxford, OX1 3PH, UK*
[b] *Department of Chemistry, University of Oxford, Oxford, OX1 3QR, UK.*
  E-mail: edman.tsang@chem.ox.ac.uk
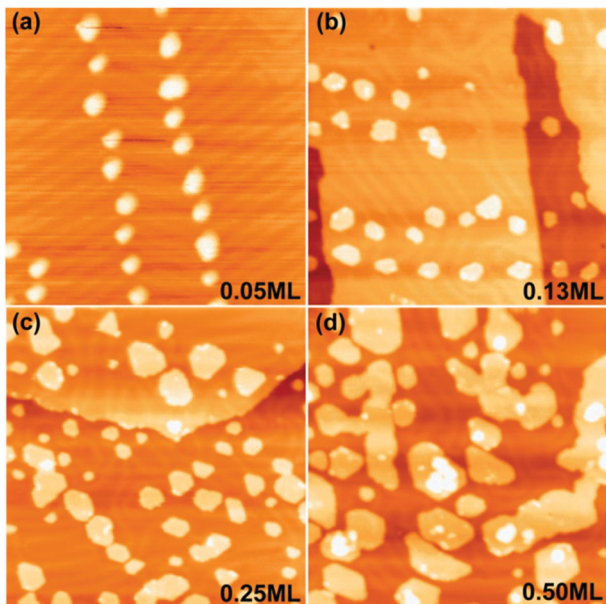
Fig. 1 STM images show Pd nanoislands on Au(111) with increasing Pd coverage: (a) 0.05 ML, 50 × 50 nm^2, U_s = −1.1 V, I_t = 0.20 nA; (b) 0.13 ML, 50 × 50 nm^2, U_s = −1.67 V, I_t = 0.12 nA; (c) 0.25 ML, 50 × 50 nm^2, U_s = −2.00 V, I_t = 0.10 nA; (d) 0.50 ML, 50 × 50 nm^2, U_s = −1.17 V, I_t = 0.25 nA.

images indeed suggests a clean Au(111) surface. The bright lines in the images of boundaries between unfaulted fcc and faulted hcp (hexagonal close-packed) stacking are clearly visible.[12] The Pd islands are seen preferentially nucleating at the elbow sites of the Au(111) reconstructions (Fig. 1), which is consistent with previous observation.[13] For samples with Pd coverage between 0.05 ML and 0.25 ML, the Pd islands exhibit a hexagonal shape, and their average sizes with narrow distributions can be measured directly from the STM images (Fig. 2b). The Pd nanoparticles coalesce with increasing Pd coverage (above 0.50 ML). Consequently, the size of the nanoparticles varies over a wide range for the 0.50 ML deposited sample. Fig. 2a shows a typical scan profile for the height variations of these images. The height of the Pd deposition is measured to be approx. 2.2 Å, which corresponds to a single atomic layer of Pd(111) deposited epitaxially on Au(111). For the 0.50 ML sample and particularly at even higher coverage, brighter features of Pd are visible in the images. Corresponding line profiles are confirmed to be double Pd atom layers (see ESI†). As a result, 0.50 ML appears to be the maximum amount of Pd deposition to create Pd islands of mostly single atom thickness.
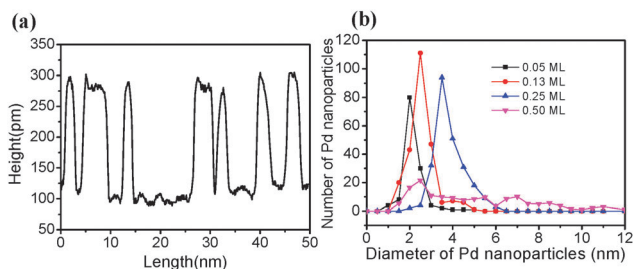
Fig. 2 (a) A line profile taken across the STM image in Fig. 1c, showing single atomic layer height of Pd islands; (b) size distribution of surface Pd islands with increasing Pd deposition.
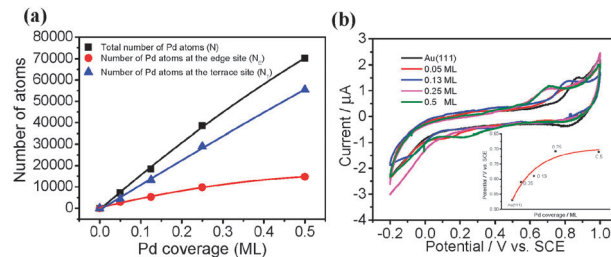
Fig. 3 (a) A plot showing trends of the total number of Pd atoms (N), Pd atoms at edge sites (N_E) and Pd on terrace sites (N_T) in a 100 × 100 nm^2 area with increasing Pd coverage; (b) cyclic voltammetry taken on samples in 0.1 M HClO$_4$ at different Pd coverages compared to clean Au(111) − the figure inset shows the degree of peak shift.

There is clear progressive coalescence of the islands at increasing Pd coverage to form irregular shapes. The total number of Pd atoms (N), the number of Pd atoms at edge sites (N_E) and the number of Pd atoms at terrace sites (N_T) on these islands are derived from the STM data (see ESI†), as shown in Fig. 3a. It is noted from the figure that the number of Pd atoms both on surface terraces and edge sites increases initially but the proportion of terrace sites becomes more dominant than that of edge sites at higher Pd coverage. We then investigated the electrocatalytic activities by CV scans of these whole mica samples mounted on a glassy carbon electrode in 0.1 M HClO$_4$ solution using a typical three electrode setup (see ESI†). Special precautions were taken in scanning the working electrodes from −0.2 to 1.0 V vs. SCE (<1.25 V to avoid surface oxide formation[14]) at a slow sweep rate of 50 mV s^{-1} to avoid kinetic dissolution of metal atoms from the surface (stable and reproducible 30–40 scans were used and averaged but long term stability of electrode surfaces was not verified) similar to the conditions adopted by Maroun et al.[8] for the electrodeposition of Pd on Au(111). An anodic peak at 0.87 ± 0.05 V is clearly observed on the mica-Au(111) surface, which is ascribed to partial electro-oxidation of the ClO$_4^-$ ion on Au(111) as

$$Au + ClO_4^- \rightarrow AuClO_4^{(1-\lambda)^-} + \lambda e^- \qquad (1)$$
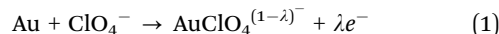
where $0 < \lambda < 1$.[14,15] Au is known to allow facilitated anodic oxidation of adsorbed perchlorate ions for this given scan range although this electron transfer may not be stoichiometric due to involvement of H-bonding with H$_2$O and other ClO$_4^-$ molecules.[15] No such oxidation peak was observed in 0.1 M H$_2$SO$_4$ or using Pd on carbon electrodes.

For all the 0.05–0.50 ML Pd samples, we did not see characteristic peaks of hydrogen absorption–desorption on the Pd surface in the range of −0.2–0.1 V (Fig. 3b). This agrees with the previous observation that Pd(111) overlayers show no sign of hydrogen absorption if they are less than 2 ML.[16] Interestingly, from the figure, we can clearly see the changes in the peak area and the peak position of this oxidation peak with Pd coverage. The peak area represents the total charge being transferred upon oxidation of hydrated perchlorate ions (see ESI†). The peak shift towards lower on-set potential (as shown in the inset of Fig. 3b.) may be induced by electronic modification of Au atoms by deposited Pd atoms on the alloy surface, which are chemically different from those in Au film or bulk Au(111).

We attempted to combine the microscopic information obtained from STM with the information derived from macroscopic
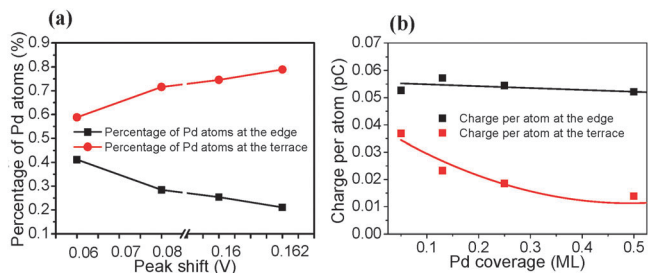
Fig. 4 (a) A plot of percentage of Pd atoms at edge and terrace sites *versus* peak shift (V). (b) A plot of peak area (charge λe^- transferred per Pd atom at terrace or edge sites) as a function of Pd coverage.

measurements of the electrochemical evaluation for the same controlled Pd deposition on Au(111) surfaces. First, the peak shift towards a lower potential with increasing Pd coverage clearly suggests that the deposited Pd atoms exert electronic effects on Au atoms for the electron transfer oxidation reaction to occur more readily. A plot of the percentage of surface terrace and edge Pd atoms with the degree of peak shift with reference to the peak (0.87 V) taken from a plain Au substrate is shown in Fig. 4a. The degree of peak shift matches well with the increasing number of surface Pd atoms at the terrace sites until levelling off (and also total Pd atoms) whilst an opposite trend is observed for Pd atoms at the edge sites. The significantly higher catalytic activity of Au atoms for electron transfer of perchlorate ions caused by neighbouring Pd atoms at lower potential could be explained by strain, ensemble and/or alloying (electronic) effects, as stated previously. The strain effect refers to the Au lattice alteration by added Pd atoms causing the change in the d-band state; the ensemble effect refers to the fact that the additional Pd may block certain sites of Au(111), reducing or eliminating the formation of an inhibiting species or an important intermediate, while the ligand effect refers to electronic modification. With respect to the strain effect for a Pd–Au surface alloy, the lattice strain is minimal with only a 4% lattice mismatch between a relaxed Pd overlayer and an Au(100) or Au(111) surface.[8] In addition, the microscopic information obtained from our STM images reveals that the most strained Au(111) atoms should be covered by the one-atom Pd ensemble hence we do not think this effect is important. Also, the clear peak shift to lower potential strongly implies the electronic effect over the ensemble effect since chemisorptive properties of a metal atom electronically modified by a dissimilar metal can differ dramatically from those of the parent bulk layer.[17] For example, the adsorption energies and dissociative reaction barriers of small molecules such as CO have been correlated with changes in the electronic properties of certain alloy overlayers.[18]

The change in the CV peak area (quantity of charge transferred from perchlorate to Au atoms at positive potential, see ESI†) could either be influenced by the Pd edge atoms or the terrace atoms. As a result, the overall charge for the electron transfer reaction per Pd atom is expressed as a terrace site or as an edge site as a function of Pd coverage and the two curves are shown in Fig. 4b, assuming that there is no intermixed contribution. It can be seen that the average charge per edge Pd atom is much higher than that of a terrace atom and is almost independent of Pd coverage (flat line). This is because the number of Pd edge atoms is much lower than terrace atoms

(see Fig. 3a) and its profile at increasing Pd coverage matches very well with the charge (peak area) profile. On the other hand, the vast number of terrace atoms and the increasing profile at Pd coverage do not seem to correlate with the observed change in total charge transferred. This may indicate that the individual Pd atoms at edge sites forming Pd–Au neighbor pairs are somehow related to the electron transfer process and thus contribute more than the latter. This is attributed to the lower coordination of Pd edge atoms and their intrinsic higher chemical reactivity to enable the peripheral Au atoms at the interface to lose electrons at positive potential during the oxidation of perchlorate ions. The curve profile of total charge per edge atom stays flat at increasing Pd coverage as the Pd–Au interface at the edge region remains almost with no change in the chemical environment despite the change in Pd edge sites at different coverages. Thus, we conclude that when more Pd islands are deposited and grow larger, the total number of the Pd atoms (or the dominant terrace sites) exert increasing electronic influence on nearby Au(111) atoms. This leads to the shift of the oxidation peak of Au(111) towards lower potential while the degree of charge transfer is dependent on the local Pd–Au neighboring pairs established at the interface. Notice that recent DFT modeling also suggests that smaller ensembles with extensive Pd–Au contact are chemically more active for adsorption reaction than monolayer films or bulk atoms.[11,19]

In summary, careful vapor controlled deposition of Pd atoms on Au(111) substrates from 0.05 ML to 0.50 ML was carried out, creating single-atom thick islands. The features are similar to those reported by Casari and co-workers with a good degree of control of surface manipulation.[13] The average size of islands, thickness and distribution of the Pd atoms can also be obtained from the STM images from which the number of Pd atoms at the edge and terrace sites is derived. Using mild scanning conditions a simple CV analysis of atomic dispersed Au(111) samples at sub-monolayer coverage can give a direct link between the microscopic structural information and the macroscopic activity evaluation. It is found that an increase in Pd deposition can facilitate electron transfer of perchlorate ions at lower anodic potential in the CV curve than pure Au(111) due to increasing ligand effect but Pd–Au neighbouring pairs at the edge interface render a higher degree of electron transfer. Thus, the electronic influence of small Pd ensembles on Au(111) atoms for electron transfer of perchlorate ions at positive potential is greater than those of higher ML films or bulk atoms. As a result, it is hoped that the present simple but fundamental study to correlate surface atom arrangements with mild testing conditions could be harnessed for future industrial catalyst design as the ultimate goal.[8,20]

Notes and references

1 Y. L. Fang, J. T. Miller, N. Guo, K. N. Heck, P. J. J. Alvarez and M. S. Wong, *Catal. Today*, 2011, **160**, 96.
2 A. M. Molenbroek, S. Haukka and B. S. Clausen, *J. Phys. Chem. B*, 1998, **102**, 10680.
3 D. I. Enache, J. K. Edwards, P. Landon, B. Solsona-Espriu, A. F. Carley, A. A. Herzing, M. Watanabe, C. J. Kiely, D. W. Knight and G. J. Hutchings, *Science*, 2006, **311**, 362.
4 J. K. Edwards, B. Solsona, N. E. Ntainjua, A. F. Carley, A. A. Herzing, C. J. Kiely and G. J. Hutchings, *Science*, 2009, **323**, 1037.
5 L. Kesavan, R. Tiruvalam, M. H. Rahim, M. I. Saiman, D. I. Enache, R. L. Jenkins, N. Dimitratos, J. A. Lopez-Sanchez, S. H. Taylor, D. W. Knight, C. J. Kiely and G. J. Hutchings, *Science*, 2011, **331**, 195.

6 T. Wei, J. H. Wang and D. W. Goodman, *J. Phys. Chem. C*, 2007, **111**, 8781.

7 M. S. Chen, D. C. Kumar, W. Yi and D. W. Goodman, *Science*, 2005, **310**, 291.

8 F. Maroun, F. Ozanam, O. M. Magnussen and R. J. Behm, *Science*, 2001, **293**, 1811.

9 V. Ponec, *Appl. Catal., A*, 2001, **222**, 31.

10 C. W. Yi, K. Luo, T. Wei and D. W. Goodman, *J. Phys. Chem. B*, 2005, **109**, 18535.

11 D. W. Yuan, X. G. Gong and R. Q. Wu, *Phys. Rev. B*, 2007, **75**, 085428.

12 J. V. Barth, H. Brune, G. Ertl and R. J. Behm, *Phys. Rev. B*, 1990, **42**, 9308.

13 C. S. Casari, S. Foglio, F. Siviero, A. Li Bassi, M. Passoni and C. E. Bottani, *Phys. Rev. B*, 2009, **79**, 195402.

14 H. Angerstein-Kozlowska and B. E. Conway, *J. Electroanal. Chem.*, 1987, **228**, 429.

15 H. Angerstein-Kozlowska and B. E. Conway, *Electrochim. Acta*, 1986, **31**, 1051.

16 M. Baldauf and D. M. Kolb, *Electrochim. Acta*, 1993, **38**, 2145.

17 J. A. Rodriguez and D. W. Goodman, *Science*, 1992, **257**, 897.

18 B. Hammer, Y. Morikawa and J. K. Norskov, *Phys. Rev. Lett.*, 1996, **76**, 2141.

19 S.-L. Peng, L.-Y. Gan, R.-Y. Tian and Y.-J. Zhao, *Comput. Theor. Chem.*, 2011, **977**, 62.

20 P. Han, S. Axnanda, I. Lyubinetsky and D. W. Goodman, *J. Am. Chem. Soc.*, 2007, **129**, 14355.